

## Article

# Development of SynBio Tools for *Pseudomonas chlororaphis*: A Versatile Non-Pathogenic Bacterium Host

Miguel Angel Bello-González <sup>1,2</sup>, Leidy Patricia Bedoya-Perez <sup>1</sup> , Miguel Alberto Pantoja-Zepeda <sup>1</sup> and Jose Utrilla <sup>1,\*</sup> 

<sup>1</sup> Centro de Ciencias Genómicas, Universidad Nacional Autónoma de México, Av. Universidad s/n Col. Chamilpa, Cuernavaca 62210, MR, México; mabello@ccg.unam.mx (M.A.B.-G.); lpbedoya@ccg.unam.mx (L.P.B.-P.); mpantoja@lcg.unam.mx (M.A.P.-Z.)

<sup>2</sup> Programa de Maestría y Doctorado en Ciencias Bioquímicas, Circuito de Posgrado, Ciudad Universitaria Universidad Nacional Autónoma de México, UNAM, Coyoacan, Mexico City 04510, México

\* Correspondence: utrilla@ccg.unam.mx

**Abstract:** *Pseudomonas chlororaphis* ATCC 9446 is a non-pathogenic bacterium associated with the rhizosphere. It is commonly used as a biocontrol agent against agricultural pests. This organism can grow on a variety of carbon sources, has a robust secondary metabolism, and produces secondary metabolites with antimicrobial properties. This makes it an alternative host organism for synthetic biology applications. However, as a novel host there is a need for well-characterized molecular tools that allow fine control of gene expression and exploration of its metabolic potential. In this work we developed and characterized expression vectors for *P. chlororaphis*. We used two different promoters: the exogenously induced lac-IPTG promoter, and LuxR-C6-AHL, which we evaluated for its auto-inducible capacities, as well as using an external addition of C6-AHL. The expression response of these vectors to the inducer concentration was characterized by detecting a reporter fluorescent protein (YFP: yellow fluorescent protein). Furthermore, the violacein production operon was evaluated as a model heterologous pathway. We tested violacein production in shake flasks and a 3 L fermenter, showing that *P. chlororaphis* possesses a vigorous aromatic amino acid metabolism and was able to produce 1 g/L of violacein in a simple batch reactor experiment with minimal medium using only glucose as the carbon source. We compared the experimental results with the predictions of a modified genome scale model. The presented results show the potential of *P. chlororaphis* as a novel host organism for synthetic biology applications.

**Keywords:** *Pseudomonas chlororaphis*; synthetic biology; violacein; vector design; host-organism; quorum-sensing; auto-induction



**Citation:** Bello-González, M.A.; Bedoya-Perez, L.P.; Pantoja-Zepeda, M.A.; Utrilla, J. Development of SynBio Tools for *Pseudomonas chlororaphis*: A Versatile Non-Pathogenic Bacterium Host. *SynBio* **2024**, *2*, 112–124. <https://doi.org/10.3390/synbio2020007>

Academic Editor: Yasuo Yoshikuni

Received: 14 December 2023

Revised: 25 January 2024

Accepted: 29 February 2024

Published: 27 March 2024



**Copyright:** © 2024 by the authors. Licensee MDPI, Basel, Switzerland. This article is an open access article distributed under the terms and conditions of the Creative Commons Attribution (CC BY) license (<https://creativecommons.org/licenses/by/4.0/>).

## 1. Introduction

Synthetic biology aims to design and engineer organisms with desired functions by applying engineering principles. To achieve this, it is essential to use host organisms that can accommodate, express, and provide the necessary cellular resources to the genetic constructs and circuits that are introduced into them. The native characteristics of organisms are considered to greatly influence their subsequent performance as emerging microbial hosts. Some of these characteristics include, but are not limited to, a range of substrate utilization, diverse metabolism, robustness, secondary metabolite production, and genomic knowledge resources [1,2]. Some of the requirements for an isolate to be proposed as a potential host organism in synthetic biology is that it be a recombinant DNA host organism, non-pathogenic, capable of accepting foreign DNA, genetically modifiable, genomically sequenced, and possibly with existing robust metabolic models, etc. [3].

Organisms belonging to the genera *Streptomyces*, *Bacillus*, *Corynebacterium*, and *Pseudomonas* have been considered as promising hosts for synthetic biology applications due to special features that make them suitable for different purposes [4]. The genus *Pseudomonas*

has many interesting features [5]. *Pseudomonas* species can adapt to many different environments and use many different substrates, and they are able to degrade contaminant compounds, to remove nitrogen in wastewater plants, and to tolerate solvents. They are natural producers of several secondary metabolites with biological activities [6]. Some members of this genus like *P. fluorescens* and *P. aureofaciens* are plant growth-promoting rhizobacteria (PGPR) [7]. The physiology of several members of the *Pseudomonas* genus has been widely studied, as it is also of medical interest for their human and plant pathogenicity and antibiotic resistance [8]. Some of the most studied *Pseudomonas* species are *P. aureoginosa*, *P. fluorescens*, *P. syringae*, *P. putida*, and *P. chlororaphis*. These species are usually found in harsh environments and are considered to be stress-tolerant [9].

*P. chlororaphis* is widely used as a biocontrol agent in different crops [10,11]. Various strains of *Pseudomonas chlororaphis* are in commercial use in the agricultural industry all over the world. Since 2011, the product “Shenqinmycin” (phenazine-1-carboxylic acid) has been put on the market in China [12]. *P. chlororaphis* strains 63–68 (commercial name: AtEze<sup>®</sup>) and TX-1 are registered as biopesticides in the United States; in Europe, there are commercial products manufactured by the company BioAgriAB using live cells of *P. chlororaphis* under the names Cedomon<sup>®</sup>, Cerall<sup>®</sup>, and Cedress<sup>®</sup>, which are used on various crops and ornamentals [13]. In recent years, an increasing number of applications have explored the potential of this organism to produce different metabolites of interest, such as phenazines [14], gentisate [15], and other antimicrobial metabolites such as Questiomycin A [16]. It has been used as a gene source for genetically modified crops [17]. The genome of this species has been completely sequenced, and a genome-scale metabolic model is also available [18]. The *Pseudomonas* Genome Database contains over 100 completely sequenced genomes and over 1450 drafts from different strains of this species [19]. Therefore, we aim to expand its application as a host for synthetic biology and metabolic engineering applications [20,21].

In this work, we developed and characterized expression tools for *P. chlororaphis* ATCC 9446. We used an external inducer and also characterized an auto-inducible system by quorum-sensing molecules. We tested our tools with the production of fluorescent proteins and a heterologous metabolic pathway. We show that *P. chlororaphis* has the potential to be a new microbial host with ample capacities due to its transformability robustness, metabolism, documented safety profile, and genomic resources generated globally by many interested research groups.

## 2. Results

### 2.1. Generation of Inducible Expression Plasmids for *P. chlororaphis*

In order to have expression tools with a tight control of gene expression, we designed two different versions of inducible plasmids. We tested the Marionette plasmids [22] that are engineered to display a tight control of gene expression. However, since these vectors carry the p15A origin of replication, they cannot replicate in *P. chlororaphis*. Therefore, we used the SEVA-631 vector that carries the BBR1 replication origin, which has been shown to be compatible with the genus *Pseudomonas* and has the gentamicin resistance marker that works in *P. chlororaphis*. We constructed six vectors (Table 1); three of these are C6-acyl-homoserine lactone (C6-AHL)-inducible and three of them are IPTG-inducible. We named these vectors SAY for the combination of SEVA and AJM vectors, with yellow fluorescent protein (YFP) as the expression reporter protein. These vectors either contain the yellow fluorescent protein (YFP) or the superfolder green fluorescent protein (sfGFP) as reporter genes. We also generated the empty versions of the plasmids that have a SapI type II restriction enzyme site to facilitate Golden Gate-compatible cloning of a gene or a pathway of interest [23]. All the generated vectors were fully sequenced, and maps are presented in Figures S1 and S2, while genebank files are presented in the Supplementary Data.

Table 1. Generated vectors.

Vector	Regulatory Element	ORF
SAY-AHL-YFP	LuxI/LuxR system (AHL)	Yellow fluorescent protein
SAY-IPTG-YFP	LacI repressor (IPTG)	Yellow fluorescent protein
SAY-AHL-sfGFP	LuxI/LuxR system (AHL)	Green fluorescent protein
SAY-IPTG-sfGFP	LacI repressor (IPTG)	Green fluorescent protein
SAY-AHL-Vio	LuxI/LuxR system (AHL)	Violacein synthesis pathway
SAY-IPTG-Vio	LacI repressor (IPTG)	Violacein synthesis pathway
SAY-AHL-SapI	LuxI/LuxR system (AHL)	Empty
SAY-IPTG-SapI	LacI repressor (IPTG)	Empty

All of the vectors share the same origin of replication BBR1, the gentamicin resistance cassette, and backbone in general.

2.2. Characterization of Induction Response of SAY Plasmids

One of the main advantages of *P. chlororaphis* as a microbial host for synthetic biology applications is its fairly high electroporation efficiency (Figure S3). To test the induction response of our SAY plasmids, we transformed *P. chlororaphis* with each plasmid and measured YFP output in glucose minimal medium across a range of inducer concentrations. As shown in Figure 1, both plasmids expressed the YFP protein and showed a dose-dependent response. The SAY-IPTG-YFP vector (Figure 1B) had a dynamic range of 0.1–1 mM, with maximum induction at 1 mM and a peak fluorescence emission of  $2.6 \times 10^5$  relative fluorescent units (RFU). Leakage of gene expression was undetected with this vector. In contrast, the SAY-AHL-YFP construct displayed a 2.69-fold higher maximum fluorescence ( $7 \times 10^5$  RFU). It displayed a higher dynamic range (0.01–1.5  $\mu$ M) but also higher transcriptional leakage due to the host organism’s ability to naturally produce the C6-AHL molecule. The sfGFP versions of the vectors were constructed for broader access of reporters; however, they were not as fully characterized as the YFP versions due to shared regulatory elements and similar results in early experiments, thus they are expected to behave in the same manner (Figure S4).

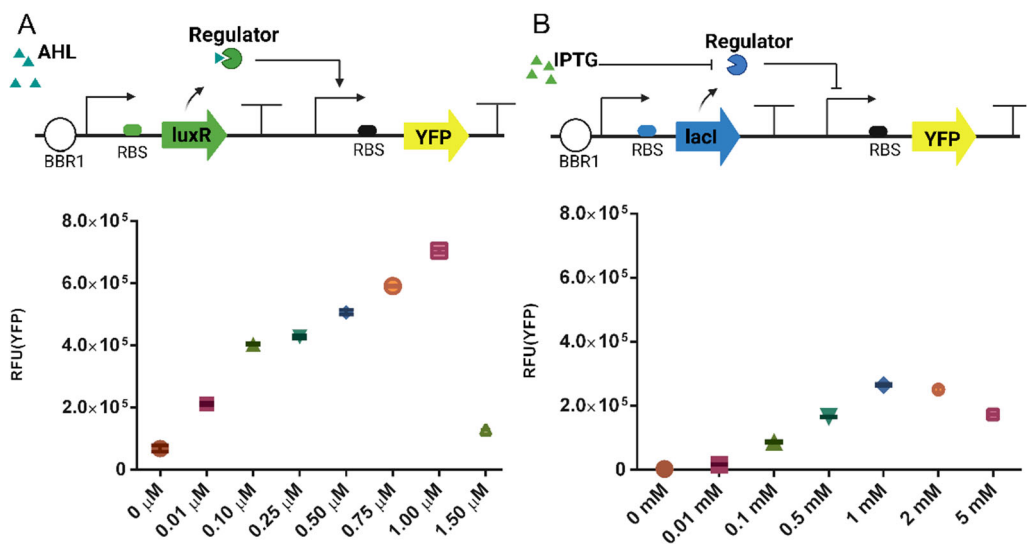
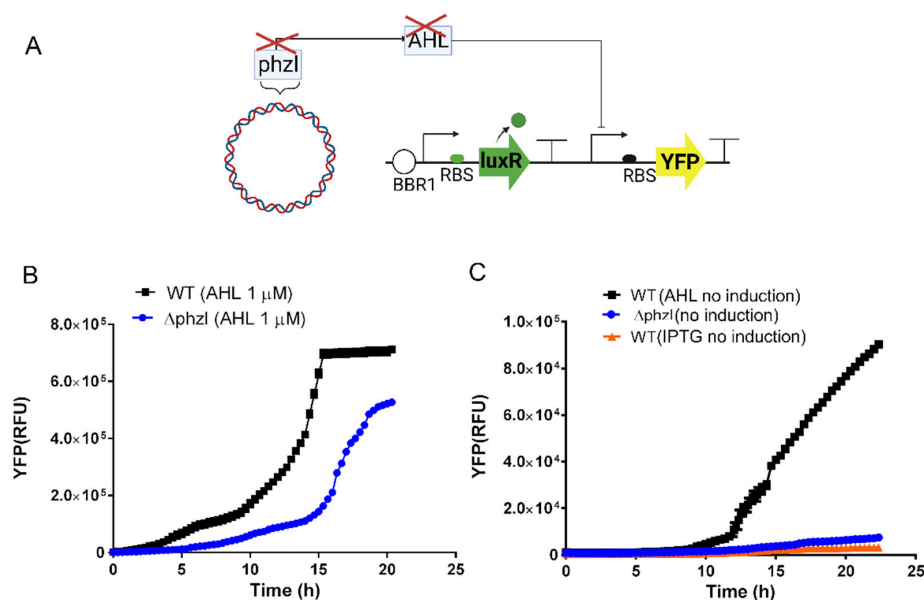


Figure 1. Plasmid design and characterization of dose response to inducer concentration. (A) Displays the organization of the SAY-AHL vector. BBR1: origin of replication, *luxR* regulators, YFP reporter gene. The chart displays the expression response of YFP, measured in relative fluorescence units (RFU),

to a gradient of concentration of exogenous C6-AHL. (B) Displays the organization of the SAY-IPTG vector. BBR1 origin of replication, lacI regulators. The chart displays the expression response of YFP, measured in RFUs, to a gradient of concentration of exogenous IPTG. Normalized data and optical density (OD) at sampling points are presented in Figure S5.

### 2.3. Quorum-Sensing Mechanisms Generate Auto-Induction in the LuxR-AHL System

*P. chlororaphis* subspecies *chlororaphis* has two luxI/luxR analogous gene complexes. The first, known as phzI (N-acyl-homoserine lactone synthase) is an AHL synthase-producing AHL, which binds to phzR (transcriptional activator) and csal (N-acyl-homoserine lactone synthase) and its regulator csaR, which are responsible for most of the synthesis of AHL molecules. These quorum-sensing (QS) molecules regulate cell-density-dependent processes and phenazine production [24,25]. The pAJM.474 vector is based on the LuxR regulator [22] activated by C6-AHL, so we expected our constructs derived from it to be sensitive to the endogenous production of AHLs. As previously shown by Morohoshi et al. [24], phzI is the main producer of AHL, and csal is the secondary producer of AHLs. Accordingly, we tested the  $\Delta$ phzI mutant and showed that it nearly abolishes all of the auto-induction (Figure 2). The mutant produces minimal YFP compared to the same strain with 1  $\mu$ M of exogenous AHL (C6-AHL) (Figure 2B). We also observed an important reduction in growth in the  $\Delta$ phzI mutant, which is probably due to pleiotropic effects, as QS molecules typically regulate the expression of many genes (Figure S6). Notably, the wild-type strain of *P. chlororaphis* can produce YFP in the same order of magnitude without an inducer; however, this production showed a 10 h delay compared to the same strain with exogenous AHL added to the medium. When comparing the normalized YFP production with an external inducer versus auto-induction, it becomes evident that experiments induced externally exhibit fluorescence production at an earlier stage of growth. This potential can be harnessed in various synthetic biology applications, when the user needs to produce early in the fermentation process or when there is the need to build up biomass to start the production stage, such as in toxic products.



**Figure 2.** Auto-induced expression mediated by AHL synthase phzI. (A) Auto-induction circuit mediated by homologous AHL synthase phzI and  $\Delta$ phzI mutant. (B) Fluorescence in *P. chlororaphis*, using exogenous addition of C6-AHL at 1  $\mu$ M on wild-type *P. chlororaphis* and  $\Delta$ phzI mutant. (C) Test of auto-induction capacity of SAY-AHL-YFP vector in wild-type (WT) and  $\Delta$ phzI mutant strains. SAY-IPTG at 0 mM induction is shown as a reference. or better data visualization, two different scales are used in Y-axis at panels (B,C).

#### 2.4. Expression of the Violacein Heterologous Pathway in *P. chlororaphis*

We tested our generated plasmids with a heterologous metabolic pathway to further characterize *P. chlororaphis* as a novel host. We used the violacein pathway, which is encoded in a five-gene operon of 7.4 kb (*vioA*, *vioB*, *vioC*, *vioD*, and *vioE* genes). Derived from its precursor, tryptophan, violacein is easily detected by its visible absorbance at 575 nM. This metabolite has interesting applications as a pigment, as well as an antibacterial, antiviral, and antiparasitic. To facilitate violacein production in various heterologous hosts, it is often necessary to supplement with a tryptophan precursor or undertake additional engineering to enhance the accessibility of tryptophan for this pathway [26]. Members of the *Pseudomonas* genus have been previously shown to have a vigorous aromatic amino acid metabolism [27]. We observed that *P. chlororaphis* was able to produce visible amounts of violacein in minimal medium with only glucose as a carbon source when transformed with our plasmids. As mentioned before, *P. chlororaphis* can use sucrose as a carbon source. Sucrose is an interesting feedstock for microbial fermentations due to its wide production in many countries, and as far as we know, *P. putida* cannot naturally use it. Therefore, we also tested sucrose in these experiments. In this case, we used our two expression systems to quantify violacein production without the supplementation of external tryptophan in shake flasks. The SAY-IPTG-Vio plasmid, induced with 1 mM IPTG, showed reduced violacein production of 143.3 mg/L, compared to the SAY-AHL-Vio construct at the maximal induction (1  $\mu$ M) that produced 742 mg/L (Figure 3). Growth profiles, measured indirectly by total protein quantification, showed that strains grow similarly (Figure S7). However, the endogenous production of AHL was not able to reach the levels of violacein that were obtained when exogenous AHL was used (Figure 3). Sucrose and glucose were used as carbon sources (Figure 3B,C). Considering the price difference between the two carbon sources, we observed that the violacein production capacity in M9-sucrose of *P. chlororaphis* was very similar to that observed in M9 with glucose. These results further demonstrate that *P. chlororaphis* is a suitable host for metabolically engineered pathways.

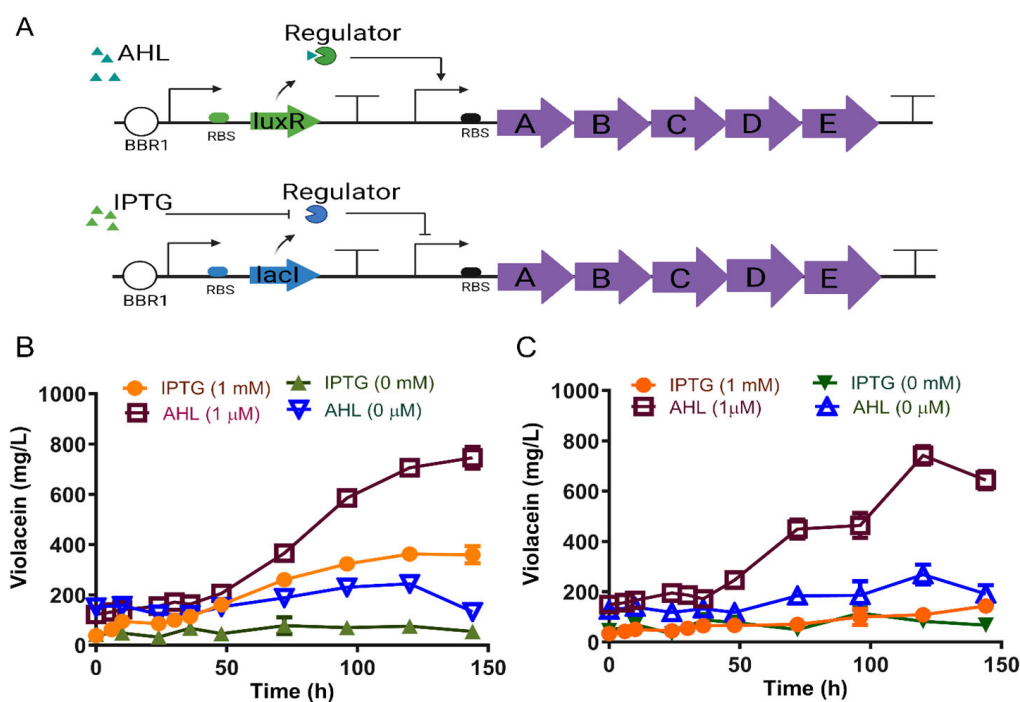


**Figure 3.** Violacein production in *P. chlororaphis*. (A) Violacein production operon in SAY-AHL-Vio and SAY-IPTG-Vio plasmids. (B) Violacein production M9 medium with sucrose 50 g/L or (C) glucose 50 g/L as the carbon source.



### 2.5. Violacein Production in a 3 L Fermenter

To show the potential of violacein production at a higher scale, with no external addition of inducer and using controlled conditions of oxygen transfer and pH, we performed a 3 L fermentation in batch mode with the *P. chlororaphis*/pSAY-AHL-Vio strain. Since we were providing a higher oxygen transfer rate and pH control, we expected to have a higher biomass production than in shake flasks. Therefore, we doubled the ammonium chloride concentration of the M9 media (18.7 mM) to ensure no nitrogen limitation occurred in these experiments. We used 50 g/L of glucose as the only carbon source. We seeded the culture with 10% preculture from a shake flask with the same medium. The results show that in this simple batch culture with no external inducer, the evaluated strain doubled the amount of total protein produced, measured as a proxy for biomass production, compared to shake flask experiments (Figure S8). The transformed strain was able to produce 989 mg/L of violacein from glucose as the only carbon source in around 60 h (Figure 4). These cultures could be further optimized to produce higher titers of violacein using changes in the media or using a feed batch strategy.

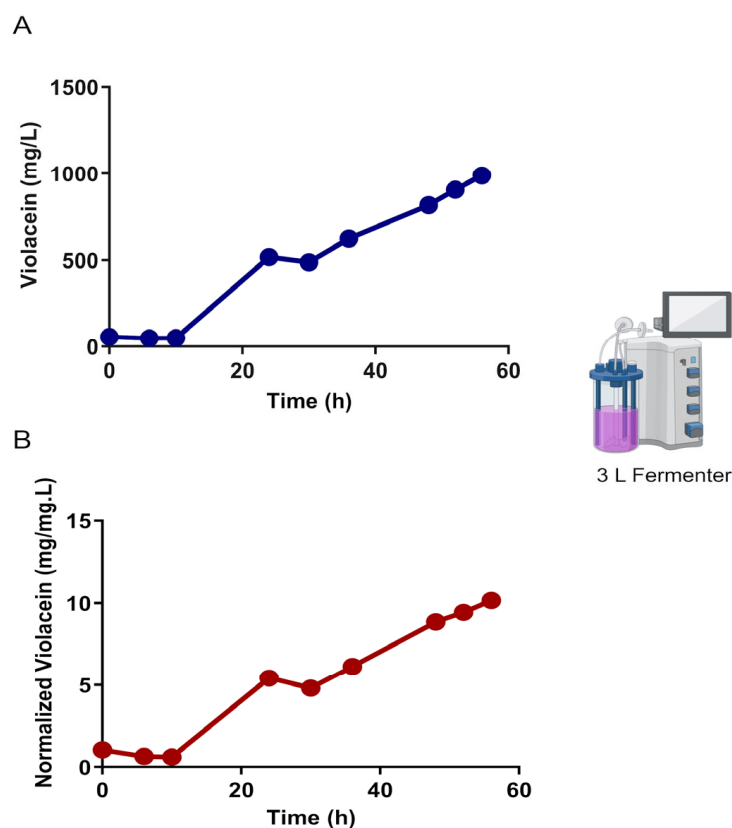


**Figure 4.** Violacein production in a 3 L fermenter in batch mode. (A) Total violacein production. (B) Normalized violacein production by measured protein.

### 2.6. Simulation of Violacein Production with a Modified iMA1267 Model

To calculate the maximum theoretical yield of violacein production from glucose in an engineered strain of *P. chlororaphis*, we first simulated the growth of the wild-type strain on glucose and sucrose at different substrate uptake rates (Figure 5B). The simulation results show that growth on sucrose, normalized by mmol C, is similar to that in glucose at the same carbon uptake rate. We also calculated the theoretical requirement of nitrogen at different carbon uptake rates, showing that the normal M9 media (9.35 mM  $\text{NH}_4\text{C}$ ) can support only up to 1.73 g of biomass. We introduced the violacein production metabolic reactions to generate a modified version of the iMA1267 model, named iMA1267\_VIO (Figure 5A). We used the glucose uptake rate measured previously [18]

and generated a production envelope to evaluate the dependency of violacein production on biomass generation (Figure 5C). We then simulated violacein production using the iMA1267\_VIO model. The maximum violacein flux is achieved at a zero-growth rate and it is 1.071442 mmol/gDCW·h, which equals a theoretical maximum yield of 0.3957 g/g of glucose. This means that using 1 g of glucose, we would expect to produce 0.3957 g of violacein. Our best production experiments are currently achieving only a small fraction of the maximum theoretical yield, indicating that there is still plenty of room for improvement in violacein production in this system.

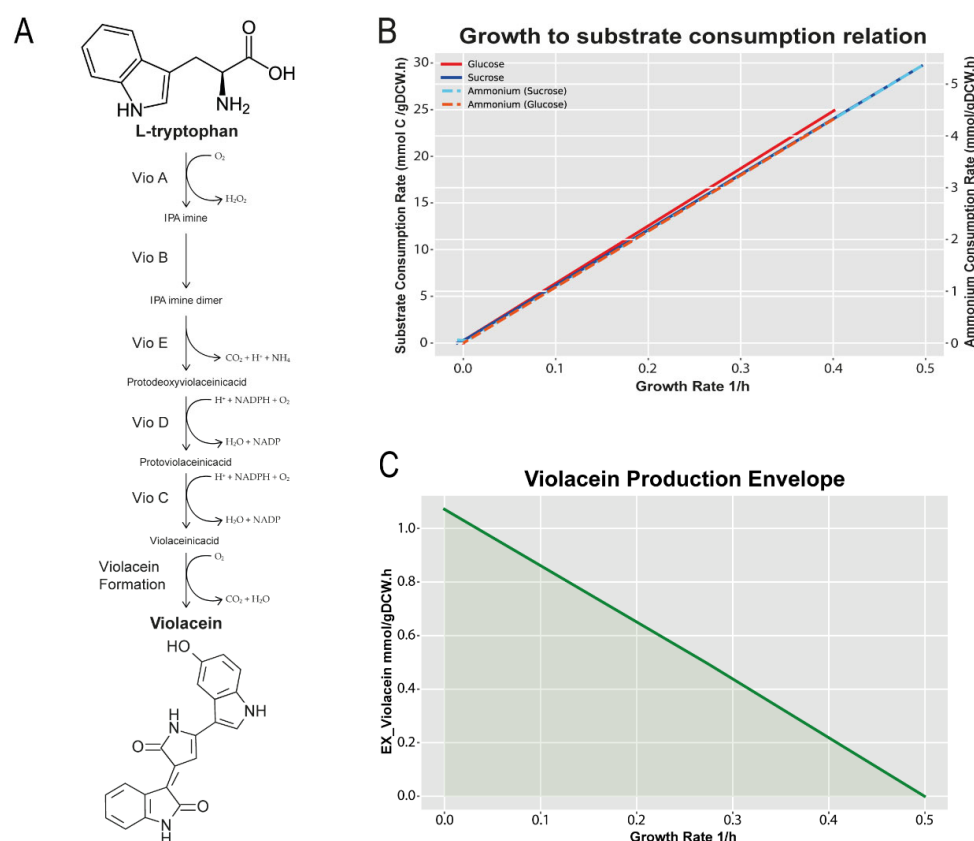


**Figure 5.** Genome scale model simulations. Simulation of growth on glucose and sucrose at different substrate uptake rates. **(A)** Pathway reconstructed in the model iMA1267\_VIO from tryptophan to violacein. **(B)** Effect of the carbon source consumption rate on the growth rate. The graph shows that with glucose (red) as the only carbon source, the growth rate is lower compared to sucrose (blue). We see how ammonium consumption in both carbon sources is very similar (light blue and yellow). **(C)** The violacein production envelope was calculated using the iMA1267\_VIO model, modified with the incorporation of the violacein pathway. Thus, the green line and the shaded area represent the potential solution area for the model's production with the production of violacein and biomass.

### 3. Discussion

The Engineering Biology Research Consortium (EBRC) has launched a roadmap for advancing the next-generation bio-economy. One of the pivotal milestones outlined in the roadmap is the broadening of microbial host choices beyond conventional model organisms [28]. *P. chlororaphis* has many advantages as a microbial host and its industrial utility in biocontrol applications has already been demonstrated, underscoring its suitability for large-scale cultivation and its safety profile as a non-pathogenic *Pseudomonas* species [17]. The present study focuses on the development of *P. chlororaphis* as a novel host for synthetic biology applications.

We developed and characterized molecular tools for controlled gene expression in *P. chlororaphis*. Our approach involved the utilization of two distinct inducers: the exoge-

nously supplied gratuitous inducer IPTG and the endogenously synthesized C6-AHL. Each of these inducers offers unique potential applications. We show that C6-AHL has the potential for auto-induction mainly mediated by the *phzI* C6-AHL synthase, as previously shown [24]. By measuring the expression of YFP under the C6-AHL/LuxR control in a wild-type strain and in a *phzI* mutant, we show that by eliminating *phzI* in *P. chlororaphis*, the auto-induction is nearly abolished. Further, we observed the highest yield of YFP production when adding 1  $\mu$ M of exogenous C6-AHL. Remarkably, the auto-induction experiments relying solely on endogenous C6-AHL still resulted in a total YFP production within the same order of magnitude as the maximum achieved with external AHL addition. We observed that even the maximal IPTG induction produces less output than C6-AHL by 2.69-fold. However, as C6-AHL is a quorum-sensing induced molecule, its exogenous addition may also affect the expression of many other genes, resulting in pleiotropic effects.

Laboratory conditions often differ from large-scale industrial conditions. Therefore, it is desirable to test more sophisticated proof-of-concepts beyond a single gene, as well as shake flask conditions, to test the true capabilities of the organisms of potential interest. The heterologous violacein production pathway is an ideal candidate to test a microbial host due to its costly five-gene pathway, and because it is potentially toxic to the production host and it is easily quantifiable. In our investigation, we assessed the viability of *P. chlororaphis* as a violacein producer using glucose and sucrose as carbon sources. Our results demonstrated that in shake flask experiments, *P. chlororaphis* yielded 742 mg/L of violacein without the need for tryptophan supplementation or any additional host strain modifications. In contrast, other heterologous hosts required tryptophan supplementation and, even then, achieved substantially lower violacein titers [26,29]. Moreover, with further optimization of the media composition and the utilization of a 3-L bioreactor, we successfully improved the production, achieving a remarkable ~1 g/L of violacein in a straightforward batch process. These findings underscore the robust potential of *P. chlororaphis* as a highly efficient microbial host for violacein and potentially other metabolically engineered products. Our simulations of violacein production with a genome scale model of *P. chlororaphis* showed that there is still great potential to improve the production yield from glucose or sucrose.

We studied the sucrose utilization potential of *P. chlororaphis*. It achieved 745 mg/L of violacein in a shake flask from the SAY-AHL-Vio plasmid. Comparing IPTG induction between glucose and sucrose, we saw higher induction using sucrose, potentially due to carbon catabolite repression [30]. Recently, the sucrose utilization potential was introduced to *P. putida* with good results [31]. Here, we show that *P. chlororaphis* ATCC 9446 has a native potential to use sucrose as a substrate in synthetic biology applications.

In this study, we demonstrate the potential of *Pseudomonas chlororaphis* as a new host for synthetic biology applications. We developed tools for controlled gene expression in two different ways. We successfully tested the production of violacein from a heterologous pathway. However, more resources are needed to advance the development of *P. chlororaphis* as a new model host, such as genomic resources [19], genome editing tools, and further developments on host physiology. A further understanding of the gene regulatory network, especially the stress tolerance mechanism, secondary metabolite production, and quorum-sensing, could be of great aid in advancing the development of this new potential microbial host.

#### 4. Materials and Methods

**Strains and growth media:** All molecular cloning protocols were performed on *E. coli* DH5-alpha strain. *P. chlororaphis* ATCC 9446 strains were used as wild-type throughout this study. *P. chlororaphis* ATCC 9446  $\Delta phzI$  was kindly donated by Dr. Gloria Soberon-Chavez [25]. LB medium and M9 medium (33.7 mM,  $\text{Na}_2\text{HPO}_4$ ; 22.0 mM,  $\text{KH}_2\text{PO}_4$ ; 8.55 mM, NaCl; 9.35 mM,  $\text{NH}_4\text{Cl}$ ; 1 mM,  $\text{MgSO}_4$ ; 0.3 mM,  $\text{CaCl}_2$ ; with trace nutrients: 13.4 mM, EDTA; 3.1 mM,  $\text{FeCl}_3\cdot 6\text{H}_2\text{O}$ ; 0.62 mM,  $\text{ZnCl}_2$ ; 76 nM,  $\text{CuCl}_2\cdot 2\text{H}_2\text{O}$ ; 42 nM,  $\text{CoCl}_2\cdot 2\text{H}_2\text{O}$ ; 162 nM,  $\text{H}_3\text{BO}_3$ ; 8.1 nM,  $\text{MnCl}_2\cdot 4\text{H}_2\text{O}$ ) was supplemented with the indicated amount of glucose or sucrose as the only carbon source. We set 250 rpm at 30 °C as



cultivation conditions. The bioreactor medium composition is the same as before but with 18.7 mM of  $\text{NH}_4\text{Cl}$ .

Generation of electrocompetent cells of *P. chlororaphis*: From an overnight culture of *P. chlororaphis* (18 h) in liquid LB medium, 1 mL was taken, centrifuged at 12,000 rpm for 1 min, and two washes of 1 mL each of a 300 mM sucrose solution were performed. Aliquots of this suspension of cells (100  $\mu\text{L}$ ) were taken and 100–200 ng of DNA were added and electroporated at 2500 V with a time constant of 4–5 milliseconds. After electroporation, the cells were recovered in 900  $\mu\text{L}$  of LB media for 1 h at 30 °C at 250 rpm, after which several dilutions were plated on LB agar medium with the corresponding antibiotic.

SAY plasmids generation: The molecular tool generation protocol was carried out by cloning desired fragments from two vectors: Marionette's pAJM.474 and pAJM.336 were a gift from Christopher Voigt (Addgene plasmid # 108526; <http://n2t.net/addgene:108526>, (accessed on 14 December 2023); RRID:Addgene\_108526), (Addgene plasmid # 108528; <http://n2t.net/addgene:108528>, (accessed on 14 December 2023); RRID:Addgene\_108528) [22] and SEVA-631 and were introduced using Gibson Assembly kit (New England Biolabs, Ipswich, MA, USA). A PCR was performed with Q5 high-fidelity polymerase to generate compatible fragments. Fragments of approximately 4.5 kb were obtained and incubated for one hour at 50 °C, following the manufacturer's specifications (Table 2).

**Table 2.** Primers and their sequence used in this study.

Primers	Use	Sequence
SEVA 631_fwd	SEVA 631 amplification for Gibson Assembly	gggtcccaataattacgatttaaatttga
SEVA 631_rev	SEVA 631 amplification for Gibson Assembly	tcctgtgtgaaattgttatccgct
AJM(AHL)_fwd	Universal primer for amplification of Marionette plasmid's for Gibson Assembly	gataacaatttcacacaggaatggctcataacacccttg
AJM(AHL)_rev	Universal primer for amplification of Marionette plasmid's for Gibson Assembly	aatcgtaattattggggaccggatgtcgcgatatag
Screening YFP FWD	Screening SEVA-AJM assembly	agggcgaggagctgttca
Screening YFP REV	Screening SEVA-AJM assembly	cttgtacagctcgtccatgc
Assembly Vio on AJM-SEVA FWD	SAY amplification for Gibson Assembly with Vio Operon	ctcggtagcaaatccagaaaagag
Assembly Vio on AJM-SEVA REV	SAY amplification for Gibson Assembly with Vio Operon	ctagtattcccctctttctagtattaaac
VioCDE_rev	pAJM.336Vio amplification for Gibson Assembly with Vio Operon	tggtaccgagtaggcgtatcacgaggcag
VioCDE_fwd	pAJM.336Vio amplification for Gibson Assembly with Vio Operon	ctaaggatcctaaggatcctactagagaagagg
VioAB_fwd	pAJM.336Vio amplification for Gibson Assembly with Vio Operon	aggatccttaggatccttaggcctctctag
VioAB_rev	pAJM.336Vio amplification for Gibson Assembly with Vio Operon	gaaatactagatgaagcattctccgatatc

After incubation, the constructs were transformed into Top10-competent cells, which were recovered in SOC medium under agitation at 37 °C for one hour. Subsequently, 100  $\mu\text{L}$  of transformed cells were seeded in LB medium with gentamicin 50  $\mu\text{g}/\text{mL}$ , where they were incubated for 24 h at 37 °C. Colony PCR was performed on a selection of the cultured colonies, and PCR-positive colonies were replicated in plates with gentamicin and the corresponding inducer to assess fluorescence production, in this case YFP. Using these

vectors as backbones, new primers were designed to clone the GFP (green fluorescent protein) reporter gene and generate new versions of SAY-GFP vectors (Table 1). All of the generated vectors were fully sequenced with Oxford Nanopore sequencing by Secoyalabs Mexico ([www.secoyalabs.com](http://www.secoyalabs.com), accessed on 14 December 2023).

**Violacein plasmids generation:** For the generation of violacein plasmids, SAY-positive plasmids were used as a template. The violacein operon was amplified from pAJM.336Vio [32] backbone in two separated fragments; fragment 1 comprised the A and B genes of the pathway, and fragment 2 the C, D, and E genes of the pathway. A three-part assembly was made according to the manufacturer's specifications and the assembly was transformed into Top10 cells.

**Fluorescence evaluation:** For fluorescence evaluation, a Synergy H1 plate reader (Biotek) was used, with measurements every 20 min for 24 h, where YFP fluorescence was evaluated at an excitation (513 nm) and emission (530 nm) wavelength. Black 96-well plates (Corning) were used for this experiment, where gradients of inducer concentrations were designed to evaluate the physiological response of *P. chlororaphis* to each inducer. IPTG (0, 0.01, 0.1, 0.5, 1, 2, 5 mM), AHL (0.01, 0.1, 0.25, 0.5, 0.75, 1, 1.50  $\mu$ M). We evaluated the physiological response in M9-glc (4 g/L) with gentamicin 50  $\mu$ g/mL. The analysis of the kinetics was performed using the Python package Fitderiv [33], and the determination of the maximum fluorescence peaks was obtained with a custom python script.

**Violacein production experiments:** M9-glucose medium (50 g/L) supplemented with gentamicin (50  $\mu$ g g/mL) was inoculated with an overnight preculture. Subsequently, the optical density OD600 was adjusted to 0.05 units and fresh M9-glucose medium was inoculated into 125 mL volume flasks containing 25 mL of M9-glucose and M9-sucrose mediums plus antibiotic. M9 was used with a sole carbon source, without tryptophan supplementation as a precursor. Samples of 500  $\mu$ L of medium were taken every 12 h for violacein and protein measurements.

**3 L Bioreactor experiments:** An inoculum of *Pseudomonas chlororaphis* transformed with the SAY-AHL-Vio vector was seeded in 100 mL of M9-glc medium (50 g/L) and incubated at 30 °C for 18 h at 250 rpm. This culture was used as the inoculum for fermentation. An Applikon Biotechnology ADI1010/1025 fermenter with 1 L working volume was used in batch culture M9 glucose medium at 50 g/L supplemented with double ammonium chloride concentration (18.7 mM) as nitrogen source and without exogenous tryptophan. Fermentation parameters were set as follows: sterile air was pumped at 1 VVM, an incubation temperature of 30 °C was used, pH was controlled to 7.0 with KOH 2N, and oxygen was controlled at 20% with a stirring cascade starting at 600 rpm.

**Violacein extraction and quantification:** Violacein was extracted by centrifugation at 12,500 rpm for 5 min, discarding the supernatant, and the pellet was suspended in 500  $\mu$ L of absolute ethanol and incubated at 95 °C for 10 min. Subsequently, another centrifugation was performed under the same conditions and the supernatant was collected. Serial dilutions were made, the absorbance was quantified in the Synergy H1 reader at a wavelength of 575 nm, and the concentration was calculated using a standard curve made with commercial violacein acquired from Sigma–Aldrich (St. Louis, MO, USA).

**Protein quantification:** Protein was extracted and quantified using the Biuret method. A solution of CuSO<sub>4</sub> at 3.2% (*w/v*) and NaOH (6 M) was used. Samples of medium with growth were centrifuged, the cell pellet was collected, and 12.5  $\mu$ L of pellet suspension was taken. 118.75  $\mu$ L of NaOH was added and incubated at 95 °C for 10 min without shaking. The sample was then allowed to warm to room temperature, 118.75  $\mu$ L of CuSO<sub>4</sub> was added, and the mixture was kept under agitation for 5 min. The tubes were then centrifuged at 13,000 rpm for 2 min. The absorbance of the samples was quantified and compared with a BSA standard curve to obtain the protein concentration.

**Genome scale modeling:** We employed the iMA1267 genome-scale model (GSMM) of *Pseudomonas chlororaphis* ATCC 9446 [18] to simulate growth and production. These simulations were conducted using the COBRApy library, version 0.25.0 [34], within a minimal M9 medium, where different carbon sources were investigated. The ATP maintenance was set

to 3.41 mmolATP/gDCWh to constrain the model [18]. Using the model.optimize() function, growth simulations were performed with varying carbon sources, specifically sucrose and glucose, to investigate the growth rates and impact on ammonium consumption (Figure 5B). The range of uptake rates for carbon sources spanned from  $-4.15$  mmol/gDCWh to zero.

To incorporate the biosynthesis pathway of violacein from tryptophan (Figure 5A) into the iMA1267 model, we extended its reactions. To generate the production envelope (Figure 5C), we utilized the reported glucose uptake rate of 5.16 mmol/gDCWh [18] as the lower bound within the minimal M9 medium.

The reactions included to simulate the production of violacein from tryptophan were defined as follows, according to the pathway depicted in Figure 5:

- (1)  $\text{o2\_c} + \text{trp\_L\_c} \rightarrow \text{h2o2\_c} + \text{ipa\_imine\_c}$
- (2)  $2 \text{ ipa\_imine\_c} \rightarrow \text{ipa\_imine\_dimer\_c}$
- (3)  $\text{ipa\_imine\_dimer\_c} \rightarrow \text{co2\_c} + \text{h\_c} + \text{nh4\_c} + \text{protodeoxyviolaceinacid\_c}$
- (4)  $\text{h\_c} + \text{nadph\_c} + \text{o2\_c} + \text{protodeoxyviolaceinacid\_c} \rightarrow \text{h2o\_c} + \text{nadp\_c} + \text{protoviolaceinacid\_c}$
- (5)  $\text{h\_c} + \text{nadph\_c} + \text{o2\_c} + \text{protoviolaceinacid\_c} \rightarrow \text{h2o\_c} + \text{nadp\_c} + \text{violaceinacid\_c}$
- (6)  $\text{o2\_c} + \text{violaceinacid\_c} \rightarrow \text{co2\_c} + \text{h2o\_c} + \text{violacein\_c}$
- (7)  $\text{violacein\_c} \rightarrow$

Initially, the product envelope for violacein production was set at zero, yielding a biomass flux of 0.4994 mmol/gDCW·h, with the glucose lower bound set to 5.16 mmol/gDCW·h. The calculated maximum theoretical yield (MTY) for violacein was 0.2075 mole of violacein per mole of glucose (0.3957 g/g of glucose).

**Supplementary Materials:** The following supporting information can be downloaded at: <https://www.mdpi.com/article/10.3390/synbio2020007/s1>. Genebank files of the plasmids and data to reproduce the figures are provided as supplementary files. Figure S1. Vector maps with fluorescent protein reporters, Figure S2. Vector maps with fluorescent protein reporters, Figure S3. Electroporation efficiency, normalized GFP measurements in kinetics of *P. chlororaphis*. Figure S4. Normalized GFP measurements in kinetics of *P. chlororaphis* wild-type strain. A. GFP measurements normalized by OD using IPTG as inductor, vector used SAY-IPTG-GFP. B. GFP measurements normalized by OD using IPTG as inductor, vector used SAY-IPTG-YFP. Figure S5. Normalized fluorescence production and OD measurements at induction gradient points, Figure S6. OD measurements in kinetics of *P. chlororaphis*  $\Delta\text{phzI}$  mutant and wild-type strain *P. chlororaphis* ATCC 9446, Figure S7. Total protein measurements with SAY-AHL-Vio vector in shake flasks, Figure S8. Total protein quantified on bioreactor.

**Author Contributions:** Conceptualization, J.U. and M.A.B.-G.; methodology, J.U., L.P.B.-P., M.A.P.-Z. and M.A.B.-G.; investigation, M.A.B.-G., L.P.B.-P. and M.A.P.-Z.; data curation, M.A.B.-G. and M.A.P.-Z.; writing—original draft preparation, M.A.B.-G. and J.U.; writing—review and editing, M.A.B.-G. and J.U.; supervision, J.U.; project administration, L.P.B.-P. and J.U.; funding acquisition, J.U. All authors have read and agreed to the published version of the manuscript.

**Funding:** This research was funded by DGAPA-UNAM, Project: IN214923.

**Institutional Review Board Statement:** Not applicable.

**Informed Consent Statement:** Not applicable.

**Data Availability Statement:** Data are contained within the article and Supplementary Materials.

**Acknowledgments:** We thank Adelfo Escalante and Alma Yolanda Alves Avilés for initial protocols, Gloria Soberón-Chavez for the kind donation of the  $\Delta\text{phzI}$  strain, and Rony Suchiapa for technical contributions. M.A.B.-G. is from the Programa de Doctorado en Ciencias Bioquímicas, Universidad Nacional Autónoma de México (UNAM), and has received a Mexican Consejo Nacional 889 de Humanidades, Ciencias y Tecnologías (CONAHCyT) fellowship, No. 867816.

**Conflicts of Interest:** The authors declare no conflicts of interest.

## References

- Hutchison, C.A.; Chuang, R.Y.; Noskov, V.N.; Assad-Garcia, N.; Deerinck, T.J.; Ellisman, M.H.; Gill, J.; Kannan, K.; Karas, B.J.; Ma, L.; et al. Design and Synthesis of a Minimal Bacterial Genome. *Science* **2016**, *351*, aad6253. [\[CrossRef\]](#) [\[PubMed\]](#)
- Wang, B.; Wang, J.; Meldrum, D.R. Application of Synthetic Biology in Cyanobacteria and Algae. *Front. Microbiol.* **2012**, *3*, 1–15. [\[CrossRef\]](#) [\[PubMed\]](#)
- de Lorenzo, V.; Krasnogor, N.; Schmidt, M. For the Sake of the Bioeconomy: Define What a Synthetic Biology Chassis Is! *N. Biotechnol.* **2021**, *60*, 44–51. [\[CrossRef\]](#) [\[PubMed\]](#)
- Sridhar, S.; Ajo-Franklin, C.M.; Masiello, C.A. A Framework for the Systematic Selection of Biosensor Chassis for Environmental Synthetic Biology. *ACS Synth. Biol.* **2022**, *11*, 2909–2916. [\[CrossRef\]](#) [\[PubMed\]](#)
- Nikel, P.I.; Martínez-García, E.; De Lorenzo, V. Biotechnological Domestication of Pseudomonads Using Synthetic Biology. *Nat. Rev. Microbiol.* **2014**, *12*, 368–379. [\[CrossRef\]](#) [\[PubMed\]](#)
- Nikel, P.I.; Chavarría, M.; Danchin, A.; de Lorenzo, V. From Dirt to Industrial Applications: Pseudomonas Putida as a Synthetic Biology Chassis for Hosting Harsh Biochemical Reactions. *Curr. Opin. Chem. Biol.* **2016**, *34*, 20–29. [\[CrossRef\]](#)
- Peng, H.; Ouyang, Y.; Bilal, M.; Wang, W.; Hu, H.; Zhang, X. Identification, Synthesis and Regulatory Function of the N-Acylated Homoserine Lactone Signals Produced by Pseudomonas Chlororaphis HT66. *Microb. Cell Fact.* **2018**, *17*, 9. [\[CrossRef\]](#) [\[PubMed\]](#)
- Elbehiry, A.; Marzouk, E.; Aldubaib, M.; Moussa, I.; Abalkhail, A.; Ibrahim, M.; Hamada, M.; Sindi, W.; Alzaben, F.; Almuzaini, A.M.; et al. Pseudomonas Species Prevalence, Protein Analysis, and Antibiotic Resistance: An Evolving Public Health Challenge. *AMB Express* **2022**, *12*, 53. [\[CrossRef\]](#)
- Rabiço, F.; Pedrino, M.; Narcizo, J.P.; de Andrade, A.R.; Reginatto, V.; Guazzaroni, M.E. Synthetic Biology Toolkit for a New Species of Pseudomonas Promissory for Electricity Generation in Microbial Fuel Cells. *Microorganisms* **2023**, *11*, 2044. [\[CrossRef\]](#)
- Tienda, S.; Vida, C.; Lagendijk, E.; de Weert, S.; Linares, I.; González-Fernández, J.; Guirado, E.; de Vicente, A.; Cazorla, F.M. Soil Application of a Formulated Biocontrol Rhizobacterium, Pseudomonas Chlororaphis PCL1606, Induces Soil Suppressiveness by Impacting Specific Microbial Communities. *Front. Microbiol.* **2020**, *11*, 548323. [\[CrossRef\]](#)
- Raio, A.; Puopolo, G. Pseudomonas Chlororaphis Metabolites as Biocontrol Promoters of Plant Health and Improved Crop Yield. *World J. Microbiol. Biotechnol.* **2021**, *37*, 1–8. [\[CrossRef\]](#) [\[PubMed\]](#)
- Liu, K.; Hu, H.; Wang, W.; Zhang, X. Genetic Engineering of Pseudomonas Chlororaphis GP72 for the Enhanced Production of 2-Hydroxyphenazine. *Microb. Cell Fact.* **2016**, *15*, 131. [\[CrossRef\]](#) [\[PubMed\]](#)
- Anderson, A.J.; Kim, Y.C. Biopesticides Produced by Plant-Probiotic Pseudomonas Chlororaphis Isolates. *Crop Prot.* **2018**, *105*, 62–69. [\[CrossRef\]](#)
- Shen, X.; Wang, Z.; Huang, X.; Hu, H.; Wang, W.; Zhang, X. Developing Genome-Reduced Pseudomonas Chlororaphis Strains for the Production of Secondary Metabolites. *BMC Genom.* **2017**, *18*, 715. [\[CrossRef\]](#) [\[PubMed\]](#)
- Wang, S.; Fu, C.; Liu, K.; Cui, J.; Hu, H.; Wang, W.; Zhang, X. Engineering a Synthetic Pathway for Gentisate in Pseudomonas Chlororaphis P3. *Front. Bioeng. Biotechnol.* **2021**, *8*, 1–10. [\[CrossRef\]](#) [\[PubMed\]](#)
- Guo, S.; Hu, H.; Wang, W.; Bilal, M.; Zhang, X. Production of Antibacterial Questionmycin A in Metabolically Engineered Pseudomonas Chlororaphis HT66. *J. Agric. Food Chem.* **2022**, *70*, 7742–7750. [\[CrossRef\]](#) [\[PubMed\]](#)
- Anderson, J.A.; Staley, J.; Challender, M.; Heuton, J. Safety of Pseudomonas Chlororaphis as a Gene Source for Genetically Modified Crops. *Transgenic. Res.* **2018**, *27*, 103–113. [\[CrossRef\]](#) [\[PubMed\]](#)
- Moreno-Avitia, F.; Utrilla, J.; Bolívar, F.; Nogales, J.; Escalante, A. Metabolic Reconstruction of Pseudomonas Chlororaphis ATCC 9446 to Understand Its Metabolic Potential as a Phenazine-1-Carboxamide-Producing Strain. *Appl. Microbiol. Biotechnol.* **2020**, *104*, 10119–10132. [\[CrossRef\]](#)
- Winsor, G.L.; Griffiths, E.J.; Lo, R.; Dhillon, B.K.; Shay, J.A.; Brinkman, F.S.L. Enhanced Annotations and Features for Comparing Thousands of Pseudomonas Genomes in the Pseudomonas Genome Database. *Nucleic Acids Res.* **2016**, *44*, D646–D653. [\[CrossRef\]](#)
- Yue, S.J.; Song, C.; Li, S.; Huang, P.; Guo, S.Q.; Hu, H.B.; Wang, W.; Zhang, X.H. Synthesis of Cinnabarinic Acid by Metabolically Engineered Pseudomonas Chlororaphis GP72. *Biotechnol. Bioeng.* **2019**, *116*, 3072–3083. [\[CrossRef\]](#)
- Wan, Y.; Liu, H.; Xian, M.; Huang, W. Biosynthesis and Metabolic Engineering of 1-Hydroxyphenazine in Pseudomonas Chlororaphis H18. *Microb. Cell Fact.* **2021**, *20*, 235. [\[CrossRef\]](#) [\[PubMed\]](#)
- Meyer, A.J.; Segall-Shapiro, T.H.; Glassey, E.; Zhang, J.; Voigt, C.A. Escherichia Coli “Marionette” Strains with 12 Highly Optimized Small-Molecule Sensors. *Nat. Chem. Biol.* **2019**, *15*, 196–204. [\[CrossRef\]](#) [\[PubMed\]](#)
- Engler, C.; Kandzia, R.; Marillonnet, S. A One Pot, One Step, Precision Cloning Method with High Throughput Capability. *PLoS ONE* **2008**, *3*, e3647. [\[CrossRef\]](#) [\[PubMed\]](#)
- Morohoshi, T.; Yabe, N.; Yaguchi, N.; Xie, X.; Someya, N. Regulation of Phenazine-1-Carboxamide Production by Quorum Sensing in Type Strains of Pseudomonas Chlororaphis Subsp. Chlororaphis and Pseudomonas Chlororaphis Subsp. Piscium. *J. Biosci. Bioeng.* **2022**, *133*, 541–546. [\[CrossRef\]](#) [\[PubMed\]](#)
- González-Valdez, A.; Escalante, A.; Soberón-Chávez, G. Heterologous Production of Rhamnolipids in Pseudomonas Chlororaphis Subsp. Chlororaphis<sup>ATCC</sup> 9446 Based on the Endogenous Production of N-acyl-homoserine Lactones. *Microb. Biotechnol.* **2023**, *17*, e14377. [\[CrossRef\]](#) [\[PubMed\]](#)
- Fang, M.Y.; Zhang, C.; Yang, S.; Cui, J.Y.; Jiang, P.X.; Lou, K.; Wachi, M.; Xing, X.H. High Crude Violacein Production from Glucose by Escherichia Coli Engineered with Interactive Control of Tryptophan Pathway and Violacein Biosynthetic Pathway. *Microb. Cell Fact.* **2015**, *14*, 8. [\[CrossRef\]](#) [\[PubMed\]](#)

27. Schwanemann, T.; Otto, M.; Wierckx, N.; Wynands, B. Pseudomonas as Versatile Aromatics Cell Factory. *Biotechnol. J.* **2020**, *15*, 1900569. [[CrossRef](#)]
28. Dixon, T.A.; Freemont, P.S.; Johnson, R.A.; Pretorius, I.S. A Global Forum on Synthetic Biology: The Need for International Engagement. *Nat. Commun.* **2022**, *13*, 3516. [[CrossRef](#)]
29. Rodrigues, A.L.; Trachtmann, N.; Becker, J.; Lohanatha, A.F.; Blotenberg, J.; Bolten, C.J.; Korneli, C.; de Souza Lima, A.O.; Porto, L.M.; Sprenger, G.A.; et al. Systems Metabolic Engineering of Escherichia Coli for Production of the Antitumor Drugs Violacein and Deoxyviolacein. *Metab. Eng.* **2013**, *20*, 29–41. [[CrossRef](#)]
30. Franzino, T.; Boubakri, H.; Cernava, T.; Abrouk, D.; Achouak, W.; Reverchon, S.; Nasser, W.; el Zahar Haichar, F. Implications of Carbon Catabolite Repression for Plant–Microbe Interactions. *Plant Commun.* **2022**, *3*, 100272. [[CrossRef](#)]
31. Löwe, H.; Sinner, P.; Kremling, A.; Pflüger-Grau, K. Engineering Sucrose Metabolism in Pseudomonas Putida Highlights the Importance of Porins. *Microb. Biotechnol.* **2020**, *13*, 97–106. [[CrossRef](#)] [[PubMed](#)]
32. Patricia Bedoya-Pérez, L.; Aguilar-Vera, A.; Sánchez-Pérez, M.; Sohlenkamp, C. Enhancing Escherichia Coli Abiotic Stress Resistance through Ornithine Lipid Formation. *bioRxiv* **2023**. [[CrossRef](#)]
33. Swain, P.S.; Stevenson, K.; Leary, A.; Montano-Gutierrez, L.F.; Clark, I.B.N.; Vogel, J.; Pilizota, T. Inferring Time Derivatives Including Cell Growth Rates Using Gaussian Processes. *Nat. Commun.* **2016**, *7*, 13766. [[CrossRef](#)] [[PubMed](#)]
34. Ebrahim, A.; Lerman, J.A.; Palsson, B.O.; Hyduke, D.R. COBRApy: CONstraints-Based Reconstruction and Analysis for Python. *BMC Syst. Biol.* **2013**, *7*, 74. [[CrossRef](#)] [[PubMed](#)]

**Disclaimer/Publisher’s Note:** The statements, opinions and data contained in all publications are solely those of the individual author(s) and contributor(s) and not of MDPI and/or the editor(s). MDPI and/or the editor(s) disclaim responsibility for any injury to people or property resulting from any ideas, methods, instructions or products referred to in the content.